Available online at www.sciencedirect.com
SCIENCE DIRECT
Polymer 47 (2006) 4571–4580
polymer
www.elsevier.com/locate/polymer

Thermosensitive poly(*N*-isopropylacrylamide)-*b*-poly(ε-caprolactone) nanoparticles for efficient drug delivery system

Changyong Choi [1], Su Young Chae [1], Jae-Won Nah *

Department of Polymer Science and Engineering, Sunchon National University, 315 Maegok, Suncheon, Jeonnam 540-742, South Korea

Received 10 January 2006; received in revised form 30 April 2006; accepted 8 May 2006
Available online 19 May 2006

Abstract

To investigate thermosensitive polymeric nanoparticle, amphiphilic block copolymers of poly(*N*-isopropylacrylamice)-*b*-poly(ε-caprolactone) (PNPCL) with different PCL block lengths were synthesized by hydroxy-terminated poly(*N*-isopropyoacrylamide) (PNiPAAm) initiated ring opening polymerization of ε-caprolactone. Owing to their amphiphilic characteristics, the block copolymers formed self-assembled polymeric nanoparticles in aqueous milieus with thermosensitive PNiPAAm shell compartment. The characterizations of the nanoparticles revealed that the PNPCL nanoparticles showed PCL block length dependent physicochemical characters such as particle sizes, critical aggregation concentrations, and core hydrophobicities. Moreover, the thermosensitive PNiPAAm shells conferred unique temperature responsive properties such as phase transitions with temperature elevation over its lower critical solution temperature (LCST). The temperature induced phase transition resulted in the formation of PNiPAAm hydrogel layer on the PNPCL nanoparticle surface. The drug release tests revealed that the formation of thermosensitive hydrogel layer resulted in the enhanced sustained drug release patterns by acting as an additional diffusion barriers. Therefore, the introduction of thermosensitive polymers on polymeric nanoparticles might be a potential approaches to modulate drug release behaviors.

Keywords: Nanoparticle; Thermosensitive; PCL

1. Introduction

Amphiphilic block copolymers, containing hydrophobic and hydrophilic chains, have been frequently studied in biotechnology and pharmaceutical fields for their unique properties of micelle or micelle-like self-aggregate formation in aqueous milieu [1–3]. Because of the limited water solubility of hydrophobic block and the hydrophobic interaction between the water-insoluble segments in aqueous environment, amphiphilic block copolymers spontaneously form micelle or micelle-like self-aggregates to achieve thermodynamic stability by minimizing interfacial free energy via intra- and/or inter-molecular segregation [2].

The self-aggregates, formed by polymeric amphiphiles, are composed with two basic compartments of hydrophobic core and hydrophilic corona. Owing to these supramolecular structure, the polymeric self-aggregates have been considered one of the promising candidates for drug carriers with higher drug concentration in an aqueous milieu than to the solubility limit of the hydrophobic free drug by partitioning the drugs into the hydrophobic core compartment [4–10]. The hydrophilic corona also endowed the polymeric self-aggregates with excellent physiological stabilities and biocompatibilities [11–13]. Therefore, a number of studies have focused on the applications of the polymeric self-aggregates into drug delivery systems [14–21]. As polymeric materials for the self-aggregate, amphiphilic block copolymers, hydrophobically modified water-soluble polymers, and hydrophobized polysaccharides have been extensively studies [22–26].

Although numerous studies and promising results of the polymeric self-aggregates as drug carriers have been reported, only few researches have been focus on the stimuli responsive polymeric nanoparticles. One of the most widely investigated stimuli sensitive polymers are poly(*N*-isopropylacrylamide) (PNiPAAm) and related copolymers [27–31]. Owing to the amphiphilic characters of the monomeric unit, the PNiPAAm shows unique reversible thermosensitivity with the hydrated extended coil to globule transition by increasing temperature over its lower critical solution temperature (LCST). The LCST of PNiPAAm in aqueous environment is around 32 °C and is dependent on its molecular weight and incorporated comonomers [32–34]. Therefore, the PNiPAAm based several block

* Corresponding author. Tel.: +82 61 750 3566; fax: +82 61 750 3508.
E-mail address: jwnah@sunchon.ac.kr (J.-W. Nah).
[1] Equally qualified as first authors.

0032-3861/$ - see front matter © 2006 Elsevier Ltd. All rights reserved.
doi:10.1016/j.polymer.2006.05.011

copolymers have been studied as temperature sensitive polymeric nanoparticles [35–41].

In this study, we focused on the poly(*N*-isopropylacrylamide)-*b*-poly(ε-caprolactone) (PNPCL) block copolymers. The hydrophobic PCL block is well-known biodegradable polyester with excellent biocompatibility and degradability. The PNiPAAm block may compose hydrophilic corona of the PNPCL nanoparticles and act as temperature sensitive component. Therefore, it is expected that the PNPCL nanoparticles might form core-shell type polymeric self-aggregates with thermosensitive nanoparticle corona. For detailed investigation, we synthesized PNPCL block copolymers with different PCL block lengths. Then, the thermosensitive PNPCL nanoparticles were prepared by solvent evaporation method and their physicochemical characteristics and thermosensitivities were investigated. Finally, the efficacies of the PNPCL nanoparticles as drug carriers were examined with the hydrophobic model drug of clonazepam.

2. Materials and methods

2.1. Materials

N-Isopropylacrylamide (NiPAAm), 2-mecrcaptoethanol (ME), 2,2′-azobisisobutyronitrile (AIBN), ε-caprolactone, stannous 2-ethyl hexanoate (stannous octoate, SnOct), pyrene, cetylpyridinium chloride (CPC), and 1,6 diphenyl-1,3,5-hexantriene (DPH) were purchased from Aldrich (St louis, MO). The NiPAAm was recrystallized in *n*-hexane. The ε-caprolactone was dried using CaH_2 for overnight and distilled under reduced pressure. The clonazepam (CNZ) was purchased from Sigma (St Louis, MO) and used as received. All other chemicals and solvents were analytical or reagent grade and used without further purifications.

2.2. Synthesis of poly(N-isopropylacrylamide) (PNiPAAm-OH) and PNPCL block copolymers

Hydroxyl terminated poly(*N*-isopropylacrylamide) (PNiPAAm-OH) was synthesized by radical telomerization using ME as a chain transfer agent with AIBN as a radical initiator. Briefly, the NiPAAm (10 g), ME (0.372 g), and AIBN (0.2 g) were dissolved in tetrahydrofuran (THF, 90 mL) and degassed under reduced pressure by triple freeze–thawing cycles. Then, the polymerization was carried out at 70 °C for 24 h with vigorous stirring. After polymerization, the reaction mixture was concentrated by solvent evaporation under reduced pressure and the polymer was obtained by precipitation in excess amount of diethyl ether. The precipitates were collected by filtration and washed twice with diethyl ether and dried in vacuo for 48 h.

Owing to the uncertainty of the chain transfer polymerization, the obtained polymer showed broad molecular weight distribution with fairly high amount of low molecular weight oligomers. Therefore, the PNiPAAm-OH was further purified by ultrafiltration to remove small molecular weight fractions. Briefly, the dried polymer was dissolved in deionized water (5 mg/mL) and the solution was filtrated through ultrafiltration membrane with molecular weight cut-offs (MWCO) of 30 kDa (using ultrafiltration stirred cell and YM30 membranes) at 4 °C. The 30 kDa membrane filtrate was further fractionated by using 10 kDa MWCO membrane, and the fraction between 30 and 10 kDa membrane was collected. Finally, separated polymers of each fractions (10–30 kDa and below 10 kDa) were obtained by lyophilization. The molecular weight of the fractionated PNiPAAm-OHs was determined by ^{1}H NMR (400 MHz, Bruker) end group analysis and gel permeation chromatography (GPC; DAWN DSP and OPTILAB DSP, Wyatt).

PNPCL block copolymers were synthesized by ring opening polymerization of ε-caprolactone using PNiPAAm-OH as initiators with a trace amount of SnOct as a catalyst. Predetermined amount of PNiPAAm-OH and toluene were introduced into a three neck flask and moisture impurities were removed by azotropic drying with removal of toluene at 120 °C. After cooling (~60 °C), one drop of SnOct and predetermined amount of ε-caprolactone were added (target PCL block lengths of 3, 5, and 7 kDa). Then, the polymerization was performed at 140 °C for 24 h with vigorous stirring. All steps were carried out in a nitrogen atmosphere. After reaction, PNPCL block copolymers were obtained by precipitation in excess diethyl ether and dried in vacuo for 48 h. The resulting PNPCL block copolymers were characterized by ^{1}H NMR and GPC.

2.3. Preparation of self-aggregated nanoparticles

PNPCL block copolymer nanoparticles were prepared by solvent evaporation method. Briefly, PNPCL block copolymers were dissolving in THF (5 mg/mL). Polymer solutions were dropped in chilled deionized water (80 mL, final concentration of polymer; 0.25 mg/mL) with sonication using probe type ultrasonic-generator (80 W). Then, THF removed by evaporation under reduced pressure. After the nanoparticle formation, the solutions were concentrated using ultrafiltration with 30 kDa MWCO membranes. Finally, the thermosensitive nanoparticles were obtained by lyophilization. The core-shell type thermosensitive PNPCL nanoparticles were characterized by ^{1}H NMR with adopting different locking solvents (D_2O and $CDCl_3$).

2.4. Measurement of thermosensitivity (lower critical solution temperature, LCST)

To measure LCSTs of PNiPAAm-OH and thermosensitive PNPCL nanoparticles, the cloud point measurement (turbidimetry) method was employed [29,30,36,38–40]. Briefly, the PNiPAAm-OH and thermosensitive nanoparticles were dispersed (0.5 mg/mL) in PBS (pH 7.4, ion strength $I=0.15$ M). The optical transmittances of these solutions were measured at 500 nm wavelength using UV–vis spectrometer (UV-1601, Shimadzu) with increasing solution temperatures (20–40 °C, 1 °C interval). At each temperature, the samples were stabilized for 10 min before measurements. Values for the

LCST of PNiPAAm-OH solution and nanoparticle dispersions were determined at a temperature with a half of the optical transmittance between blow and above transitions.

2.5. Nanoparticle characterizations (DLS and FEG-SEM)

The particle size and the size distribution of the thermosensitive nanoparticles were investigated by dynamic light scattering (DLS, Otsuka, ELS 8000) equipped with an argon laser operating at 632.8 nm with a fixed scattering angle of 90°. Before measurement, the nanoparticles were re-dispersed in deionized water (1 mg/mL), sonicated for 30 s, and filtered through a 0.8 μm pore size filter to remove large aggregates. Measurements were carried out at higher concentration than the critical aggregation concentration (CAC) obtained by fluorescence spectroscope. The hydrodynamic diameters of the thermosensitive nanoparticles were calculated by the Stokes–Einstein equation, and the polydispersity factors represented as μ_2/Γ^2 were evaluated form the cummulant method (μ_2; second cummulant of the decay function, Γ^2; average characteristic line width).

The morphologies of the thermosensitive nanoparticle were investigated by a field emission gun scanning electron microscopy (FEG-SEM, S-4300, Hitachi, Japan). To make specimen, a drop of the nanoparticle suspension was placed on a graphite surface and dried by lyophilization. After drying, the sample was coated with platinum/palladium using an Ion Sputter (12–15 mA for 80 s, E-1010, Hitachi). Finally, the observation was performed at 5 kV.

2.6. Measurement of fluorescence spectroscopy (pyrene and DPH)

The self aggregation behaviors of the PNPCL copolymers were investigated by fluorescence measurements using pyrene as a hydrophobic fluorescence probe. Briefly, the pyrene solution in acetone (6×10^{-5} M, prepared prior to use) was added to the deionized water to make a pyrene concentration of 1.2×10^{-6} M, and the acetone was removed at reduced pressure at 40 °C for 2 h. This solution was mixed with block copolymer solutions to make copolymer concentration from 2.0 to 1.0×10^{-5} mg/mL, resulting in a pyrene concentration of 6×10^{-7} M. Pyrene fluorescence spectra were obtained by using spectrofluorophotometer (RF-5301PC, Shimadzu, Japan). Fluorescence excitation spectra were measured at the emission wavelength $\lambda_{em}=390$ nm. Slit width was set at 3 nm for the excitation. Based on the pyrene excitation spectra and red shift of the spectra (major peak, 335–338 nm) with increasing PNPCL concentrations, the critical aggregation concentrations of the PNPCLs were measured.

The aggregation number of PCL block per one hydrophobic micro-domain was determined by the steady state fluorescence quenching method with CPC as a pyrene fluorescence quencher [42]. In microheterogeneous systems such as aqueous self-aggregate solution of amphiphilic block copolymers, the probe fluorescence intensity is dependent upon concentration of the quenching molecule in the system ([Q]). The steady state quenching data is widely accepted to fit in the quenching kinetics as follows

$$\ln\left(\frac{I_0}{I}\right)=\frac{[Q]}{[M]} \tag{1}$$

where I_0 and I are the fluorescence intensity with the absence and presence of a quencher, [Q] is the concentration of the quencher, and [M] is the concentration of hydrophobic microdomains in the solution. Therefore, the number of hydrophobic group (PCL blocks in this system) in a hydrophobic microdomain (N_{PCL}) can be calculated by Eq. (2).

$$N_{PCL}=\frac{[\text{PCL block}]}{[M]} \tag{2}$$

The temperature sensitive physicochemical characters, especially the nanoparticle hydrophobicities, were investigated by dye solubilization method with DPH as microenvironment sensitive fluorescence dye [43–45]. Briefly, the DPH stock solution (20 μL, 0.4 mM in methanol) was added to 2 mL of nanoparticle solutions (3×10^{-4}–2 mg/mL) and left in the dark for 3 h for equilibrium. Then, 100 μL samples were placed into 96 well plate and their absorption intensities at 356 nm (characteristic peak point of DPH) were obtained with a microplate reader (VERSAman, Molecular Device, CA, USA) at various temperatures (25–43 °C). By using the obtained absorption data, CMC values at each temperature were calculated by the crossover point at low concentration ranges.

2.7. Drug loading and release test

To investigate the efficacy of the thermosensitive PNPCL nanoparticles as drug carrier, hydrophobic model drug of clonazepam (CNZ) was loaded into the nanoparticles and drug release patterns were studied. To prepare drug loaded PNPCL nanoparticles, solvent evaporation method was employed. Briefly, 20 mg of PNPCL block copolymer and 4 mg CNZ were dissolved in 5 mL of THF. Then, the solution was slowly added into 80 mL of chilled deionized water with mile sonication (80 W) by using probe type ultrasonic generator. After formation of CNZ loaded polymeric nanoparticles, the organic solvent was removed by evaporation under reduced pressure. The nanoparticle suspension was concentrated by ultrafiltration apparatus equipped with 30,000 molecular weight cut-off membrane (with ultrafiltration stirred cell, final volume around 10 mL). Finally, the concentrated nanoparticle solution was filtered through 0.8 μm pore sized syringe filter and CNZ loaded nanoparticles were obtained by lyophilization.

To measure drug content and loading efficiency, the CNZ loaded nanoparticles were dissolved in DMF (0.01 mg/mL). The solution was centrifuged and supernatant was taken for measurement of drug concentration using UV–vis spectrophotometer at 322 nm. Drug contents and loading efficiency were calculated (Eqs. (3) and (4)).

$$\text{Drug contents}=\frac{A}{A+B}\times100 \tag{3}$$

Where, A and B are the weight of remained drug in the nanoparticles and polymer weight, respectively

$$\text{Loading efficiency} = \frac{C}{D} \times 100 \quad (4)$$

Where, C and D are the amount of remained drug in the nanoparticles and initial feeding amount of drug, respectively.

The in vitro drug release experiment was carried out as described previously [46]. Briefly, 4 mg of CNZ loaded polymeric micelles was dispersed into 1 mL of PBS (pH 7.4, I: 0.15 M), which was put into a dialysis membrane (MWCO: 12000) and the membrane were immersed into vials containing 30 mL PBS. Then, the drug release tests were performed at two different temperatures (25 and 37 °C) with continuous shaking (shaking water bath, 100 rpm). During the drug release test, whole media was withdrawn and replaced with fresh buffer solution at each sampling points in order to prevent the reach of saturation concentration of drug in the solution. The concentration of the released CNZ in the samples was determined by UV–vis spectrometer.

3. Results and discussions

3.1. Characterizations of PNiPAAm-OH and PNPCL block copolymers

The hydroxyl terminated PNiPAAm-OH was synthesized by radical chain-transfer polymerization. Although the chain-transfer polymerizations have been frequently employed for synthesis of low molecular weight telechelic polymers, the resulting PNiPAAm-OH showed broad molecular weight distributions owing to the inhomogeneous initiation and chain transfer reactions. Furthermore, the low MW fractions also seriously affected the thermosensitivity of PNiPAAm by increasing its LCST values. Therefore, the low MW PNiPAAm oligomers were removed by ultrafiltration techniques. As illustrated in Fig. 1, the GPC chromatograms clearly showed the efficacy of separation steps. Before fractionation, the

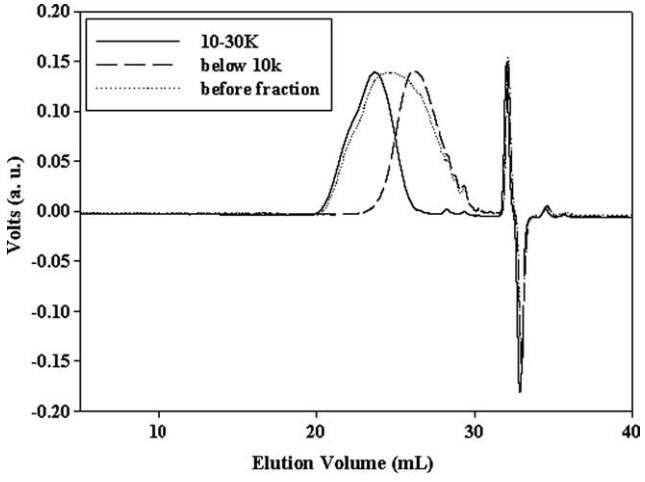

Fig. 1. GPC spectra of PNiPAAm-OH and its fractionated products. The synthesized PNiPAAm-OH was separated by ultrafiltration and the fractionated products showed two different average MWs of 7600 Da (solid line) and 1100 Da (medium dashed line). Dotted line represents raw PNiPAAm-OH.

PNiPAAm showed average MW (M_n) of 2400 with high polydispersity index values (M_w/M_n) of 2.192. However, two separated fractions showed narrow molecular weight distributions with number average molecular weight of 7600 and 1100 Da by 10–30 K fraction and below 10 K fraction, respectively. The LCST values of these PNiPAAm-OHs obtained by turbidimetry also showed similar patterns. In case of unfractionated PNiPAAm, the LCST value was 35.5 °C. However, those of 10–30 K fraction and below 10 K fraction were 34.6 and 48.5 °C, respectively. Therefore, the 10–30 K fraction was utilized for ε-caprolactone polymerization. The 10–30 K fraction was further characterized by ^{1}H NMR spectrometer using D_2O as a locking solvent. The chemical shift of the PNiPAAm-OH was followed. PNiPAAm-OH ^{1}H NMR (D_2O, ppm, TMS); 3.61 ppm (polymer end, HOCH_2CH$_2$S-PNiPAAm), 3.88 ppm (g in Fig. 2, –CH(CH$_3$)$_2$), and 1.08 ppm (f in Fig. 2, –CH(CH_3)$_2$). Degree of polymerization of PNiPAAm-OH also calculated using the integration values. The M_n of PNiPAAm-OH was 8000 Da.

The PNPCL block copolymers were confirmed by ^{1}H NMR spectra. The ^{1}H NMR spectra of PNPCL block copolymers showed the co-existence of characteristic peaks of PNiPAAm and PCL blocks (Fig. 2). PNPCL block copolymers ^{1}H NMR ($CDCl_3$, ppm, TMS): 3.98 ppm (g in Fig. 2, –CH(CH$_3$)$_2$ in PNP), 1.19 ppm (f, –CH(CH_3)$_2$ in PNP), 1.21–2.58 ppm (PNP main chain CH– and –CH_2–), 2.48 ppm (a, –OCOCH_2(CH$_2$)$_4$– in PCL), 2.65 ppm (b, –OCOCH$_2$CH_2CH$_2$CH_2CH$_2$– in PCL), 1.38 ppm (d, –OCOCH$_2$CH$_2$CH_2CH$_2$CH$_2$– in PCL), and 4.05 ppm (e, –OCOCH$_2$CH$_2$CH$_2$CH$_2$CH_2– in PCL). The M_n values and PCL block length were calculated based on integration values of each block copolymers and listed in Table 1. PCL block lengths were 830, 1920 and 5350 Da, respectively. The average MWs and polydispersity values of PNPCL block copolymers also measured by GPC and the results were listed in Table 1.

3.2. Characterizations of the PNPCL thermosensitive nanoparticles

The amphiphilic block copolymer can self-aggregate to form nanoparticles consist of hydrophobic core and hydrophilic shell in aqueous milieus. For PNPCL block copolymers, the formation of hydrophobic PCL domain can easily be confirmed by ^{1}H NMR spectra with $CDCl_3$ and D_2O as locking solvents. The results, as demonstrated in Fig. 2, showed that in $CDCl_3$, a nonselective solvent for PNiPAAm and PCL blocks, the completed structural resolution of each blocks were observed (Fig. 2(A)). However, in D_2O, only the PNiPAAm signals were detected, which mainly originated from the selective solvation of exterior hydrophilic PNiPAAm shell through hydrogen bond formation with D_2O (Fig. 2(B)). The results revealed that the PCL blocks in PNPCL block copolymers were formed hydrophobic domain in the nanoparticles and remained in solid and/or semi-solid state, which resulted in the disappearance of PCL characteristic peaks in D_2O. Similar trends of ^{1}H NMR spectra are consistent with

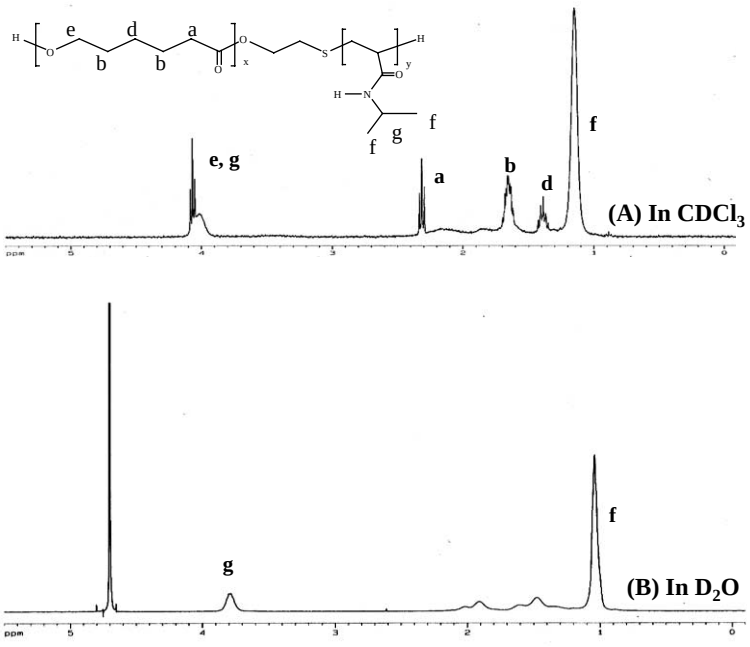

Fig. 2. ^{1}H NMR spectra of PNPCL85 in (A) D_2O and (B) $CDCl_3$, and peak assignment of the synthesized copolymer.

Table 1
Characterizations of the synthesized PNPCL block copolymers

Sample	PNP MW (K)	PCL MW (K)[a]	PCL MW[b]	PCL wt%[b]	M_n[b]	M_n[c]	PDI[c]
PNPCL83[d]	8	3	830	9017	9050	8974	1.412
PNPCL85	8	5	1920	18.93	10,140	10,410	1.301
PNPCL87	8	7	5350	39.43	13,570	13,270	1.346

[a] Theoretical PCL MW based on feed ratio.
[b] Calculated from ^{1}H NMR data.
[c] Number average M_n and polydispersity index by GPC.
[d] PNPCL83, PNP8K-block-PCL3K.

other amphiphilic block copolymer systems and hydrophobized polysaccharides [2].

PNiPAAm is one of the most widely invested thermosensitive polymer with highly hydrated extended coil to globule transition upon heating. The transition resulted in the precipitation and/or sol to gel transformation of PNiPAAm or related copolymers. The transition phenomena can be easily characterized by optical property change (turbidimetry) of polymeric solution or hydrogels containing PNiPAAm. In this research, the PNiPAAm and PNPCL block copolymers showed optical property (transmittance at 500 nm) changes upon heating, as illustrated in Fig. 3. The transmittance changes were closely relied with PCL block length. By decreasing PCL block length, the more sharp and dominant transmittance reductions were observed. Based on the Fig. 3 data, the LCSTs were determined at a temperature with a half of the optical transmittance change between below and above the transitions. The LCSTs were in the range of 29.5–35.2 °C and the results were summarized in Table 2.

The mean diameters of PNPCL block copolymer nanoparticles, measured by DLS, were in the range of 45–210 nm (Table 2). Furthermore, spherical morphology of micelles was

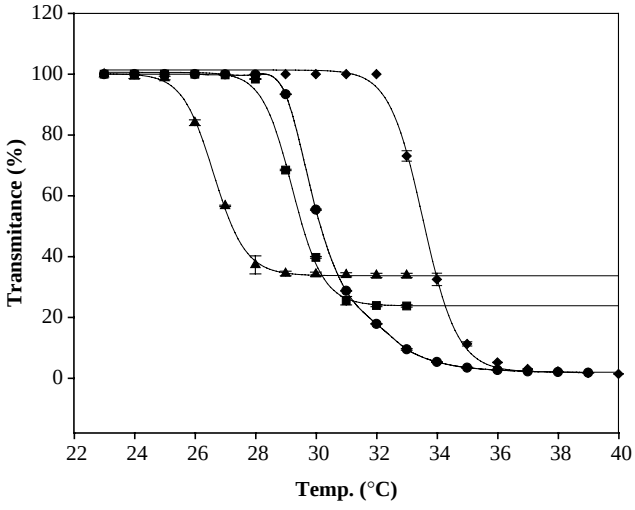

Fig. 3. Measurement of the transmittance of PNiPAAm and PNPCL nanoparticles in PBS at $\lambda = 500$ nm. (●; PNPCL83, ■; PNPCL85, ▲; PNPCL87, and ♦; PNiPAAm-OH).

Table 2
Characterizations of the PNPCL nanoparticles by DLS and fluorescence probe method

Samples	x_{PCL}[a]	LCST[b] (°C)	CAC (mg/L)	K_v[c] (10^{-5})	N_{PCL}[d]	d (nm)	Polydispersity (μ_2/Γ^{-2})
PNPCL83	0.092	32.2	5.605	4.7	99	45	0.3134
PNPCL85	0.189	30.6	2.833	6.0	82	145	0.2884
PNPCL87	0.394	29.5	1.614	8.1	46	210	0.2523

[a] PCL weight fraction calculated from ^{1}H NMR data.
[b] Measured by UV (PNP LCST:34.6 °C).
[c] Binding equilibrium constant of pyrene in water in the presence of the PCPCL nanoparticles.
[d] Aggregration number of PCL blocks per on hydrophobic microdomain.

established by FEG-SEM and the size was similar to DLS results (Fig. 4). The particle size increased as the PCL block length increased. The increment of particle size with increasing PCL block length is mainly originated from the increase of hydrophobic property by the longer hydrophobic PCL chain in aqueous milieu. These phenomena were closely agreed with our previous examinations [47].

To investigate the self-aggregation behaviors of PNPCL block copolymers in aqueous milieus, photophysical properties of the nanoparticle solution was investigated using hydrophobic fluorescence probe of pyrene. With exposure to polymeric self-aggregate aqueous solution, pyrene molecules preferably participate into inside or close to the hydrophobic microdomains of the self-aggregate rather than in aqueous phase. The localization, combined with strong fluorescence illumination of pyrene in a non-polar environment, shows the different photo-physical characteristics depending on the concentration of self-aggregate forming materials [2,48,49]. Therefore, the self-aggregation behaviors of the PNPCL block copolymers aggregates were investigated by using fluorescence excitation spectra of the PNPCL block copolymers aggregated solutions with various concentrations, in the presence of 6.0×10^{-7} M pyrene. At low concentration ($c<$CAC), there were negligible changes in total fluorescence intensity. As increasing concentration, remarkable increase of the total fluorescence intensity and a red shift of the (0,0) band from 335 to 338 nm were observed. Fig. 5 shows the intensity ratio (I_{338}/I_{335}) of the pyrene excitation spectra versus the logarithm of the PNPCL block copolymers concentrations. Based on the intensity ratio data, the CAC values of PNPCL block copolymers were calculated by the crossover point at low concentration ranges. The CAC values of PNPCL block copolymers, as summarized

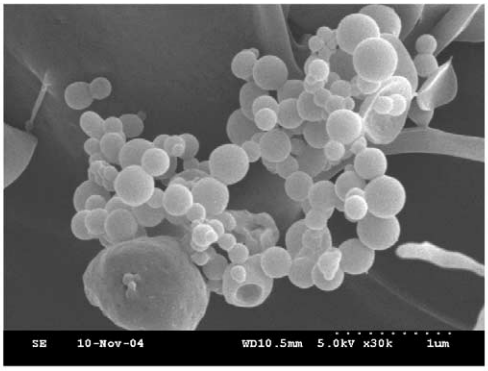

PNPCL83

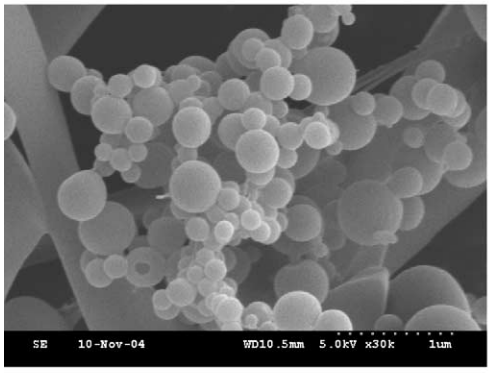

PNPCL85

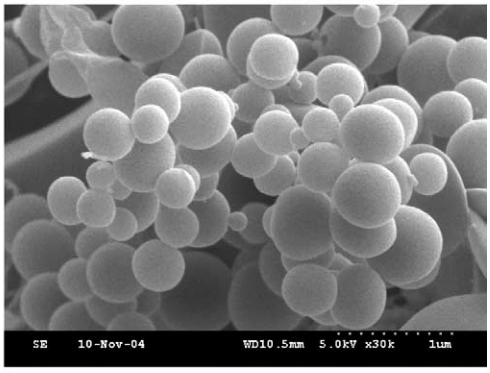

PNPCL87

Fig. 4. Image of PNPCL nanoparticles obtained with a FEG-SEM.

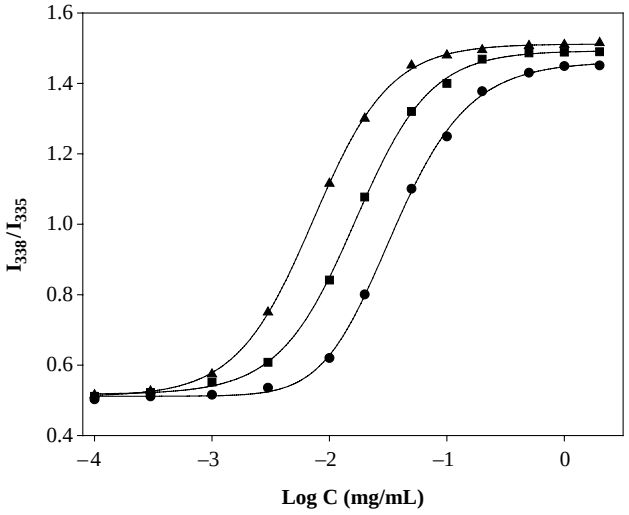

Fig. 5. Plot of total fluorescence excitation intensity ratio (I_{338}/I_{335}) versus PNPCL block copolymers concentrations. (●; PNPCL83, ■; PNPCL85, and ▲; PNPCL87).

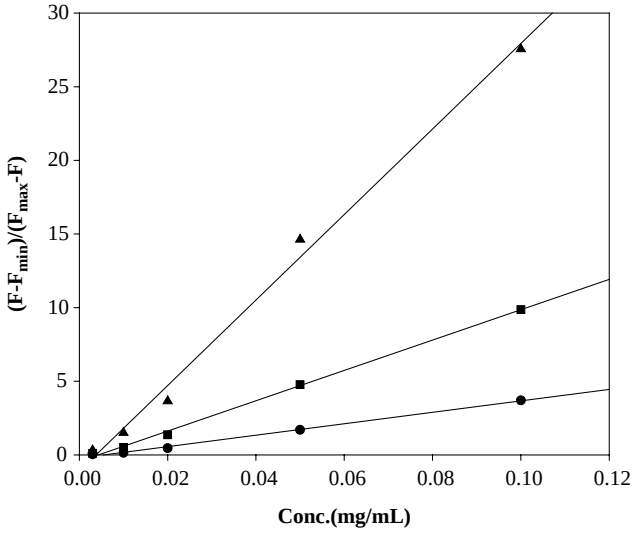

Fig. 6. Plot of $(F-F_{min})/(F_{max}-F)$ versus PNPCL block copolymers concentrations. Solid lines indicate the best fit to the data according to Eq. (5). (●; PNPCL83, ■; PNPCL85, and ▲; PNPCL87).

Table 2, were in the range of 1.614–5.605 mg/L. The CAC values from pyrene emission spectra showed similar trends (data not shown). These results reveled that the block copolymer with longer PCL block length requires small amounts of it for forming of the self-aggregate. The CAC values of PEGCLs were similar to the reported values of amphiphilic block copolymers such as PEG–PLA, poly (2-ethyl-2-oxazoline)–PCL, and PVP–PCL block copolymers [48,50,51].

The hydrophobic characteristics of interior microdomain of PNPCL block copolymer self-aggregates were investigated by estimating the pyrene equilibrium constant (K_v), which is originating from the localization of pyrene between aqueous and hydrophobic microdomain. With assumption of simplified equilibrium state, the molar ratio of pyrene in the micellar phase to the water phase can be expressed as following equation

$$\frac{[\mathrm{Py}]_m}{[\mathrm{Py}]_w} = \frac{K_v V_m}{V_w} \tag{5}$$

where V_m and V_w are the micellar and water phase volumes, respectively. In micellar association sensitive case, the Eq. (5) can be expressed as

$$\frac{[\mathrm{Py}]_m}{[\mathrm{Py}]_w} = \frac{K_v x_{PCL}(c-\mathrm{CAC})}{1000\rho_{PCL}} \tag{6}$$

where x_{PCL} is the weight fraction of PCL block, c is the concentration of the PNPCL block copolymer and ρ_{PCL} is assumed a the bulk density of PCL (1.043–1.146 in Aldrich catalogue, adopt the average value of 1.10). In the intermediate range of PNPCL block copolymer concentration, $[\mathrm{Py}]_m/[\mathrm{Py}]_w$ values can be calculated by

$$\frac{[\mathrm{Py}]_m}{[\mathrm{Py}]_w} = \frac{(F-F_{min})}{(F_{max}-F)} \tag{7}$$

where F_{max} and F_{min} are the intensity ratio (I_{338}/I_{335}) at high and low polymer concentration ranges, and F is the intensity ratio in the intermediate concentration range.

The pyrene equilibrium constant (K_v) can be easily calculated from the slopes of $(F-F_{min})/(F_{max}-F)$ versus polymer concentration graph (Fig. 6). The K_v values, summarized Table 2, were in the range of $4.7–8.1\times10^5$. The K_v values increased with increasing PCL block length. These results reveled that the hydrophobicity of the core of self-aggregates was increased. Resultantly, the block copolymer with longer hydrophobic PCL blocks can entrap more amount of hydrophobic materials into the self-aggregates.

To determine the aggregation number of PCL chains in a hydrophobic microdomain, self-aggregates were investigated by using a fluorescence quenching method with various

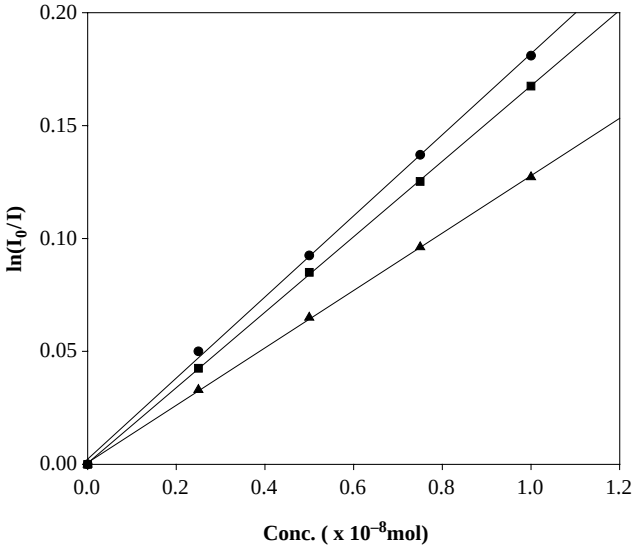

Fig. 7. Plot of fluorescence intensity $\ln(I_0/I)$ versus CPC quencher concentration. (●; PNPCL83, ■; PNPCL85, and ▲; PNPCL87).

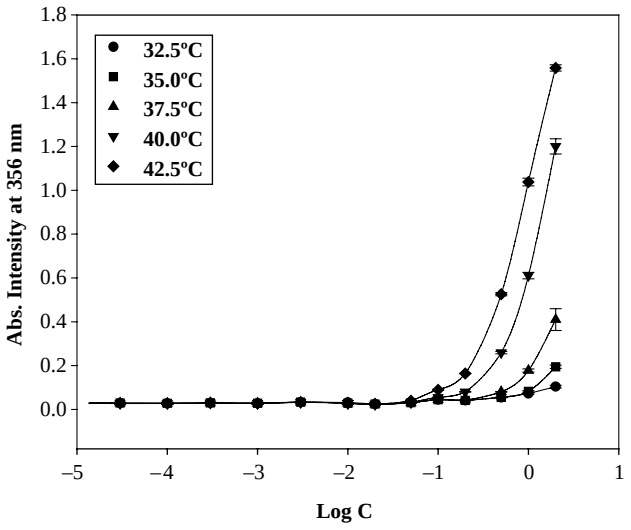

Fig. 8. Effects of concentration, with various temperatures, on the absorption intensity of DPH at 356 nm in aqueous solution of PNPCL83.

quencher concentration. As shown in Fig. 7, the $\ln(I_0/I)$ versus CPC concentration plots showed linear relationships. The aggregation numbers of PNPCL block copolymers can be calculated using slope of the straight line using Eq. (2). The aggregation numbers of PCL blocks in a hydrophobic microdomain were in the range of 46–99 as summarized in Table 2. The results revealed that the copolymers with longer hydrophobic PCL block required relatively small number of PCL block to form a hydrophobic microdomain than block copolymer with shorter PCL block. In comparison with particle size and K_v values, the copolymers with short PCL block may form nanoparticles with a few number of hydrophobic microdomain.

One of the most characteristic features of the PNPCL nanoparticles is their temperature sensitivity originated from PNiPAAm shell. The temperature responsive phase transition of PNiPAAm shell also resulted in the alternation of the PNPCL nanoparticle physicochemical properties. As illustrated in Fig. 8, the DPH dye solubilization patterns of PNPCL83 nanoparticles were closely related with polymer concentration and experimental temperature. Based on the Fig. 8 results, the CAC values of the PNPCL nanoparticles at different temperatures were calculated and listed in Table 3. Although the CACs measured by dye solubilization method showed different values, which obtained by pyrene fluorescence spectroscopy, the results clearly showed that the CAC values of PNPCL nanoparticles seriously affected by the experimental temperatures owing to the PNiPAAm phase transition. In case of PNPCL83 nanoparticles, the CAC value of 0.8318 mg/mL at 32.5 °C was continuously reduced and reached 0.1259 at 42.5 °C measurement. Similar reduction of CAC values were measured by PNPCL85 and PNPCL87 nanoparticles. Other polymeric materials showing reverse thermosensitivity such as pluronic copolymers, PEG–PLGA–PEG, and PEO–PLLA block copolymers showed similar CAC reduction with temperature induced phase transitions [43–45].

Table 3
CAC of PNPCL nanoparticles aqueous solutions as a function of solution temperature

Temperature (°C)	CAC (mg/mL)		
	PNPCL83	PNPCL85	PNPCL87
32.5	0.8318	0.4266	0.2884
35.0	0.7586	0.3548	0.2344
37.5	0.3162	0.2239	0.1585
40.0	0.1995	0.1202	0.0933
42.5	0.1259	0.0794	0.0537

3.3. Drug loading and release studies

The amphiphilic block copolymers and their nanoparticles have been frequently employed for drug carrier [3,5,15–17,19]. In this study, the thermosensitive PNPCL nanoparticles were also investigated as drug carrier after loading of hydrophobic model drug of CNZ. As preliminary study, the effect of the drug/carrier ratio on the drug loading efficiency and drug content were investigated. The drug/carrier ratio of 1/10 and 2/10 showed similar drug loading efficiencies. However, further increment of the drug/carrier ratio (the ratio of 3/10) resulted in the formation of large aggregates and precipitated by products. Therefore, further experiments were carried out the fixed drug/carrier weight ratio of 2/10. As listed in Table 4, CNZ loaded PNPCL nanoparticles showed slightly increased particle sizes than original forms (without drug) and the particle sizes were in the range of 170–250 nm. During the drug loading, the PNPCL block copolymers showed excellent characteristics for drug carriers owing to their high drug loading efficiencies (72.6–95.1%) and drug contents (15.8–19.2%). The drug loading efficiencies and drug contents also showed a general trend of increasing these efficacies with PCL block length increment.

One of the main foci on this research is investigation of stimuli responsive, especially temperature sensitive polymeric nanoparticles a efficient drug carrier. To investigate the effect of polymer compositions and environmental temperatures on drug release behaviors, the drug release tests were performed at two different temperature of 25 °C (below PNiPAAm LCST) and 37 °C (above PNiPAAm LCST) with three different CNZ loaded PNPCL nanoparticles. As illustrated in Fig. 9, the CNZ loaded PNPCL nanoparticles showed well-developed sustained drug release patterns with a trend of slower drug release with increased PCL block lengths. In case of 25 °C release tests (Fig. 9(A)), the drug

Table 4
Characterization of clonazepam loaded PNPCL nanoparticles

Sample	Polymer (mg)	Drug (mg)	Drug content (%)	Loading efficiency (%)	d (nm)
PNPCL83	20	4	15.78	72.6	170
PNPCL85	20	4	18.77	93.4	250
PNPCL87	20	4	19.23	95.1	250

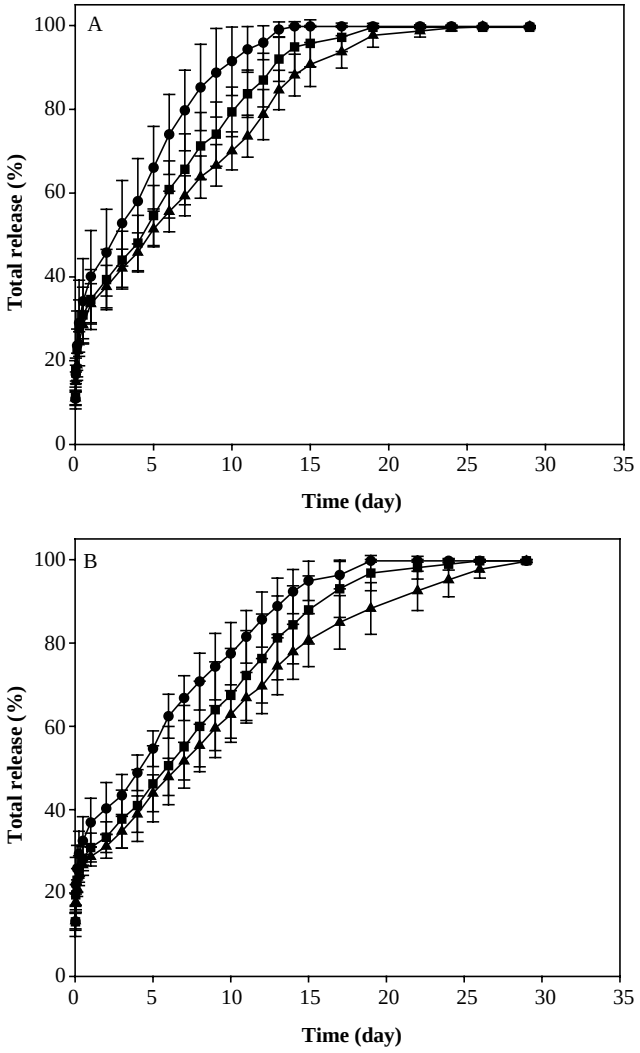

Fig. 9. Total drug (clonazepam) release behavior from nanoparticles at 25 °C (A) and 37 °C (B). (●; PNPCL83, ■; PNPCL85, and ▲; PNPCL87).

releases were completed (>95% release) at 12 and 20 days after incubation from PNPCL83 and PNPCL87 nanoparticles, respectively. The release tests performed at 37 °C also showed similar drug release patterns (Fig. 9(B)). The effect of PNiPAAm hydrogel layers on the nanoparticle surface by temperature phase transition also affected drug release patterns (at 37 °C). Owing to the increase of hydrophobicity of the PNPCL nanoparticle shell compartments, the sustained drug release patterns were increased and the drug release of PNPCL87 nanoparticles were completed at 30 days after incubation. Therefore, it is possible to conclude that the formation of PNiPAAm hydrogel layer might be act as additional diffusion barrier for the drug release.

4. Conclusion

In the present study, the thermosensitive amphiphilic PNiPAAm–PCL block copolymers (PNPCLs) with different PCL block lengths were synthesized and their nanoparticles were evaluated as stimuli sensitive drug carriers. Owing to the amphiphilic character, the PNPCL block copolymers formed self-aggregated nanoparticles and the nanoparticles showed excellent potentials for drug carriers. Furthermore, the PNiPAAm shell showed temperature induced phase transition at slightly lower than physiological temperature with enhancement of nanoparticle hydrophobicities. Furthermore, drug release test revealed that the formation of PNiPAAm hydrogel layers on the nanoparticle surfaces delayed the drug release patterns by acting as an additional diffusion barrier. Therefore, the introduction of thermosensitive polymers on polymeric nanoparticles might be a useful approach to enhance and/or modulate drug release patterns.

Acknowledgements

This study was supported by National Research Laboratory (NRL) Project from the Ministry of Science and Technology in Korea, and Research Foundation of Engineering College of Sunchon National University (2005).

References

[1] Hubbell JA. Science 2003;300:595–6.
[2] Kwon S, Park JH, Chung H, Kwon IC, Jeong SY, Kim I. Langmuir 2003; 19:10188–93.
[3] Kataoka K, Harada A, Nagasaki Y. Adv Drug Delivery Rev 2001;47: 113–31.
[4] Shenoy D, Little S, Langer R, Amiji M. Pharm Res 2005;22(12): 2107–14.
[5] Kim SY, Lee YM, Kang JS. J Biomed Mater Res A 2005;74(4):581–90.
[6] Zhang Y, Zhuo R. Biomaterials 2005;26(33):6736–42.
[7] Mainardes RM, Evangelista RC. Int J Pharm 2005;290:137–44.
[8] Panyam J, Willams D, Dash A, Leslie-Pelecky D, Labhasetwar V. J Pharm Sci 2004;93(7):1804–14.
[9] Hu Y, Jiang X, Ding Y, Zhang L, Yang C, Zhang J, et al. Biomaterials 2003;24:2395–404.
[10] Chawla JS, Amiji MM. Int J Pharm 2002;249:127–38.
[11] Ruan G, Feng SS. Biomaterials 2003;24(27):5037–44.
[12] Brus C, Petersen H, Aigner A, Caubayko F, Kissel T. Bioconjugate Chem 2004;15(4):677–84.
[13] Yamamoto Y, Nagasaki Y, Kato Y, Sugiyama Y, Kataoka K. J Controlled Release 2001;77:27–38.
[14] Xu JP, Ji J, Chen WD, Shen JC. J Controlled Release 2005;107:502–12.
[15] Venkatraman SS, Jie P, Min F, Freddy BY, Leong-Huat G. Int J Pharm 2005;298:219–32.
[16] Opanasopit P, Yokoyama M, Watanabe M, Kawano K, Maitani Y, Okano T. Pharm Res 2004;21(11):2001–8.
[17] Zeng F, Liu J, Allen C. Biomacromolecules 2004;5:1810–7.
[18] Cho H, Chung D, Jeongho A. Biomaterials 2004;25:3733–42.
[19] Zhou S, Deng X, Yang H. Biomaterials 2003;24:3563–70.
[20] Liggins RT, Burt HM. Adv Drug Deliv Rev 2002;54:191–202.
[21] Rosler A, Vandermeulen GW, Klok HA. Adv Drug Deliv Rev 2001;53: 95–108.
[22] Francis MF, Piredda M, Winnik FM. J Controlled Release 2003;93: 55–68.
[23] Yoo HS, Lee JE, Chung H, Kwon IC, Jeong SY. J Controlled Release 2005;103:235–43.
[24] Jung SW, Jeong YI, Kin SH. Int J Pharm 2003;254:109–21.
[25] Akiyoshi K, Kobayashi S, Shichibe S, Mix D, Baudys M, Kim SW, et al. J Controlled Release 1998;54:313–20.

[26] Kwon IC, Kim YH, Jeong SY. Macromolecules 1998;31:378–83.
[27] Zhang XZ, Wang FJ, Chu CC. J Mater Sci Mater Med 2003;14: 451–5.
[28] Zhang X, Wu D, Chu CC. Biomaterials 2004;25:4719–30.
[29] Verestiuc L, Ivanov C, Barbu E, Tsibouklis J. Int J Pharm 2004;269: 185–94.
[30] Kim S, Healy KE. Biomacromolecules 2003;4:1214–23.
[31] Makino K, Hiyoshi J, Ohshima H. Colloids Surf, B: Biointerfaces 2001; 20:341–6.
[32] Jeong B, Bae YH, Lee DS, Kim SW. Nature 1997;388:860–2.
[33] Jeong B, Kim SW, Bae YH. Adv Drug Deliv Rev 2002;54:37–51.
[34] Vernon B, Kim SW, Bae YH. J Biomed Mater Res 2000;51:69–79.
[35] Neradovic D, Soga O, Van Nostrum CF, Hennink WE. Biomaterials 2004;25:2409–18.
[36] Kohori F, Sakai K, Aoyagi T, Yokoyama M, Sakurai Y, Okano T. J Controlled Release 1998;55:87–98.
[37] Uchida K, Sakai K, Ito E, Kwon OH, Kikuchi A, Yamato M, et al. Biomaterials 2000;21:923–9.
[38] Chung JE, Yokoyama M, Aoyagi T, Sakurai Y, Okano T. J Controlled Release 1998;53:119–30.
[39] Chung JE, Yokoyama M, Yamato M, Aoyagi T, Sakurai Y, Okano T. J Controlled Release 1999;62:115–27.
[40] Kohori F, Sakai K, Aoyagi T, Yokoyama M, Yamato M, Sakurai Y, et al. Colloids Surf, B: Biointerfaces 1999;16:195–205.
[41] Kohori F, Yokoyama M, Sakai K, Okano T. J Controlled Release 2002; 78:155–63.
[42] Turro NJ, Yekta A. J Am Chem Soc 1978;100:5951–2.
[43] Alexandrides P, Holzwarth JF, Hatton TA. Macromolecules 1994;27: 2414–25.
[44] Jeong B, Lee DS, Shon JI, Bae YH, Kim SW. J Polymer Sci, Part A: Polym Chem 1999;37:751–60.
[45] Jeong B, Bae YH, Kim SW. Colloids Surf, B: Biointerfaces 1999;16: 185–93.
[46] Jeon HJ, Jeong YI, Jang MK, Park YH, Nah JW. Int J Pharm 2000;207: 99–108.
[47] Choi C, Chae SY, Kim TH, Jang MK, Cho CS, Nah JW. Bull Korean Chem Soc 2005;26(4):523–8.
[48] Han SK, Na K, Bae YH. Colloids Surf, A: Physicochem Eng Aspects 2003;214:49–59.
[49] Wilhelm M, Zhao CL, Wang Y, Xu R, Winnik MA, Mura JL, et al. Macromolecules 1991;24:1033–40.
[50] Lee SC, Chang Y, Yoon JS, Kim C, Kwon IC, Kim YH, et al. Macromolecules 1998;32:1847–52.
[51] Lele BS, Leroux JC. Macromolecules 2002;35:6714–23.